Nanoscale

PAPER

View Article Online
View Journal

Cite this: DOI: 10.1039/d6nr00608f

Novel liquid–liquid interface deposition method for thin films of two-dimensional solids

Amy R. Smith, Muhammad Zulqurnain,†‡ Angus G. M. Mathieson,‡ Marek Szablewski * and Michael R. C. Hunt *

Received 11th February 2026,
Accepted 27th May 2026

DOI: 10.1039/d6nr00608f

rsc.li/nanoscale

Thin films and van der Waals heterostructures (vdWHs) derived from two-dimensional solids offer enormous potential for a broad range of novel, energy efficient devices, however their use is currently hampered by slow, labour-intensive fabrication methods often employing hazardous chemicals. We demonstrate a liquid–liquid interface technique for rapid, low-cost, and low environmental impact production of ultra-thin films and vdWHs of two-dimensional solids from aqueous surfactant-stabilised suspensions. The approach is generic to two-dimensional materials which can be stabilised in aqueous suspension by a surfactant and the resulting films can be transferred to an arbitrary substrate by a range of approaches. The wide applicability of this technique is demonstrated through production of thin films on a variety of substrates, deposition of transparent, highly conductive few-layer graphene films with conductivities between 7.7×10^3–1.26×10^5 S m^{-1} and transmittances of 55–75%, and by the fabrication of a vdWH of MoS_2, WS_2, and few-layer graphene.

1 Introduction

Thin films of two-dimensional (2D) solids and van der Waals heterostructures (vdWHs) derived from them offer enormous potential for a broad range of applications, including transistors,[1–5] solar cells,[6,7] and functional devices and coatings.[8–13] vdWHs leverage the lack of dangling bonds at the surface of a 2D solid to produce atomically-abrupt and defect-free interfaces without the constraints of lattice-matching demanded by conventional heterostructures.[14] Novel structures based on 2D building blocks can, in principle, be assembled arbitrarily. However, in practice, methods of producing thin films and vdWHs of 2D materials are often difficult to scale and can be environmentally unfriendly.

Micromechanical exfoliation is frequently used to produce very high quality materials particularly suited to fundamental studies. However, the need to mechanically 'peel' monolayer or few-layer platelets from the corresponding bulk solid, transfer to a solid substrate through direct contact[3] and identify[15] the monolayer/few layer material present among unwanted multilayer flakes is inherently time consuming. In addition this technique requires considerable skill, can be difficult to reproduce and is impractical to scale to large area films.[16] These issues become even more pronounced in producing vdWHs.[17,18] Chemical vapour deposition (CVD),[19] another commonly reported approach to producing high-quality thin films of two-dimensional layered materials (2DLMs), is more rapid but suffers from a high energy budget and requires specific process parameters for each film composition. Moreover, CVD possesses a limited ability to produce vdWHs due to intermixing between layers which often occurs during growth,[20] has applicability only to certain substrates which must be robust enough to be able to withstand the growth temperatures employed, and often requires pre- or post-treatment of substrates.[21]

Solution processing is a particularly attractive route, however many liquid suspension based fabrication approaches require chemical modification of the 2D materials.[6,22,23] Such modification, even if 'reversed', usually results in a high concentration of defects.[24] Moreover, chemical modification routes have a lack of generalizability across the various different 2DLMs.[25] Film and heterostructure deposition by solution processing[5] is, in principle, applicable to a wide range of 2DLMs and substrates. Film formation may be achieved through inkjet printing,[26] spin-coating[27] or previously reported liquid–liquid interfacial film assembly approaches.[28–36] However, many of the previously reported methods suffer from multiple steps and the use of often harmful chemicals associated with the production of 2DLM inks/suspensions, coupled with the need to tailor the precursor ink/suspension formulation approach to each specific 2DLM used.

The liquid–liquid interface assembly approach developed by Woltornist and co-workers has successfully produced a

Department of Physics, Durham University, South Road, Durham, DH1 3LE, U.K.. E-mail: marek.szablewski@durham.ac.uk, m.r.c.hunt@durham.ac.uk
†Current address: Department of Physics, Cavendish Laboratory, University of Cambridge, Cambridge, CB3 0HE, U.K.
‡These authors contributed equally to this work.

range of few-layer 2DLMs stabilised at the interface between immiscible organic and water phases without chemical modification or the use of surfactants.[12,29,31,36–41] The exfoliation and segregation of 2DLM platelets to the interface of the solvents is driven thermodynamically through reduction in the high interfacial surface energy associated with the pristine aqueous/organic interface and the large energy cost associated with motion of the 2DLM into either liquid phase.[12,29] Assembly of 2DLMs at interfaces has also been exploited starting with pre-prepared suspensions,[28,32,34] by direct injection of 2DLMs[34] or through a 'bottom up' process using precursor reagents at the interface.[42] Such interfacial trapping approaches have been employed to produce composite foams and gels,[12,38,39,41] membranes,[40] and thin films.[29,31–33,35,36,43] However, there has been, to the best of our knowledge, no previous demonstration of the deposition of vdWHs, as opposed to heterogeneous single layer films[32] by liquid–liquid interfacial deposition.

Here we report a novel modification to liquid–liquid interface deposition, distinct from previously reported methods,[29,30,32,34,44] for the controllable formation and deposition of monolayer and few-layer films of 2D solids and van der Waals heterostructures derived from them. The complete end-to-end process, which we term 'Liquid Interface Deposition' (LID), is simple and rapid, taking approximately 7 hours from starting solid bulk 'parent' raw materials to deposited film (see SI Table S1 for comparison with other methods). The process of deposition from precursor materials typically takes of order one hour. LID is scalable, removes surfactants/thicker material, minimises the use of hazardous chemicals, and recycles process chemicals. LID enables deposition of films of 2D materials on substrates without prior surface treatment, employing a surfactant-stabilised aqueous suspension of thin platelets of the 2D solid as a precursor. Moreover, by successive deposition vdWHs may be rapidly produced, which, to the best of our knowledge, is the first demonstration of the deposition of vdWHs by liquid–liquid interfacial deposition. We include data from a vdWH fabricated by our method as a proof-of-principle demonstration of heterostructure production. The technique reported here is applicable to any 2D solid which can be dispersed in surfactant-stabilized aqueous suspension and therefore includes the vast majority of those materials which do not require a substrate or other external 'scaffold' or support for stability (*e.g.*, two-dimensional layered materials (2DLMs) such as graphene, transition metal dichalcogenides (TMDCs), hexagonal boron nitride (hBN) *etc.*[5,14]).

The LID method performs three roles: first, the assembly of a thickness-controlled film of platelets of a 2D solid at the interface of two immiscible liquids, which can then be readily transferred onto a substrate through dipping, as discussed here (other transfer approaches such as horizontal dipping, pouring, or freeze transfer are discussed in the SI, section S1, Fig. S1–3); second, the removal of platelets of undesirable (*i.e.*, multilayer) thickness from the film, if present in the initial surfactant-stabilised suspension; finally and crucially, the removal of surfactant from the platelets, forming a 'clean', uncontaminated film of the 2D solid(s). Vertical vdWHs are formed by repeating the process multiple times using different 2D solids without measurable disruption to previously deposited layers. The LID approach reported here has significant advantages over previously reported liquid–liquid interfacial assembly and deposition mechanisms,[29,30,32,34] with its rapidity, the capacity to remove surfactants/contaminants, and broad applicability (see SI Table S1 for comparison with other methods). Moreover, both the production of precursor suspension and the deposition method are readily scaled to mass production,[45,46] have a low energy budget (estimated to be a few percent of that required for CVD, for example), require little specialised equipment or technical know-how, can be adapted to minimise waste and environmental impact, and no direct chemical modification is made to the 2D solids in any part of the process.

2 Experimental

2.1 Production of surfactant-stabilised aqueous 2DLM suspensions

Surfactant-stabilised aqueous suspensions of 2DLMs were produced by a common approach through high shear exfoliation of a 'parent' layered 3D solid in ultra-pure water (Milipore-Q, 18.2 MΩ cm) in the presence of a surfactant. For the work presented here either Triton X-100 (Sigma Aldrich) or Tween 20 (Sigma Aldrich) was used, although any surfactant which meets the criterion of having a high partition coefficient into the non-aqueous phase should be suitable. Shear exfoliation of the 2DLM parent material was performed using a Silverson L5M shear mixer at speeds between 2000–9000 rpm, corresponding to shear rates of 23–104 kHz. The resulting suspension was then centrifuged (Eppendorf 5804) to eliminate thicker and larger platelets from the suspension.[47,48] Surfactant-stabilised aqueous suspensions of graphene, MoS_2, and WS_2 were produced from their as-received bulk parent materials (Alfa Aesar, Sigma Aldrich).

2.2 LID thin film deposition

For thin film and vdWH deposition, an aqueous precursor surfactant-stabilized suspension (approximately 2 ml) was added to a 50 ml centrifuge tube containing approximately 22.5 ml of a 'separation solvent', dichloromethane (DCM). An emulsion of the surfactant-stabilised aqueous suspension and DCM (Fisher Scientific, 99.8+%) was produced by shaking, using a vortex mixer (Vortex-Genie 2). The colour of the emulsion was dependent on the precursor material (*e.g.*, grey for graphene, green for MoS_2). The emulsion was placed in an ultrasonic bath until a clear separation between the immiscible liquids was observed. The sample was then centrifuged for 25 minutes at 11 000 rpm (corresponding to a relative centrifugal force of 16 639*g*),[49] leading to the formation of a thin continuous film at the interface between the two immiscible phases. The previously coloured aqueous suspension which lay above the interface became clear and consisted only of pure water, to the limit of detection with UV-vis (Cary 5000 UV-Vis-NIR

Spectrophotometer, Shimadzu UV-3600 UV-Vis-NIR Spectrophotometer) and Raman (ASEQ RM1, 532 nm, 10× objective, power ~18 mW cm^{-2}) spectroscopies. Below the interface the phase consisted of a solution of Triton X-100 in DCM with small aggregates of thick 2DLM platelets at the bottom of the centrifuge tube. The centrifuging step is not essential but accelerates the surfactant removal and liquid–liquid interface film assembly: if the centrifuge tube containing the DCM and aqueous suspension is left to settle over approximately 24 hours, the surfactant will migrate across the interface into the DCM and a film will form at the interface between the two liquids. Scaling of the process can therefore be achieved *via* using larger centrifuges or large tanks for gravitationally-driven assembly.

Once formed at the interface between the two immiscible liquids the film was transferred to a variety of substrates, both hydrophobic and hydrophilic, by dipping, or by other methods discussed in the SI. Analysis using Raman spectroscopy of the thin films and heterostructures showed no evidence of the presence of the surfactant, separation solvent, or any other contaminants, indicating that the film formation process simultaneously removed the surfactant and other sources of gross contamination. There was also no evidence of surfactant when performing scanning electron microscopy (Zeiss Sigma 300 VP) or TEM analysis of samples. Deposition through dipping was found to be the most versatile and effective approach and is hence discussed in detail here, with the results of the other techniques reported in the SI section S1.

The 2DLM platelets used for the production of films have a maximum area of ~60 μm^2 and a maximum lateral extent of ~7 μm (a typical size distribution is shown in SI, Fig. S4 and S5). Platelet size distributions were determined by vacuum filtering an aliquot of the surfactant-stabilised aqueous suspension onto cellulose nitrate (Whatman, pore size 0.1 μm) filter membranes. The few-layer 2DLM platelets were thoroughly washed in ultrapure water and then imaged with a scanning electron microscope using backscattered electrons. The resultant images were then analyzed to determine metrics related to platelet dimensions, including the distribution of area and lateral size, using custom-developed code. Typically, >3500 platelets were used to determine size distributions. Full details of the semi-automated platelet characterization method will be reported elsewhere (in preparation, A. R. S., M. S., M. R. C. H.).

2.3 Film and heterostructure characterisation

The transmittance of thin films and vdWHs deposited on transparent substrates was measured using UV-Vis-NIR spectroscopy, using the same apparatus used to characterise the liquid phases, described above. The uniformity of deposition was measured using a CanoScan LiDE 200 flatbed scanner, following the approach of De *et al.*,[50] with transmittance calibrated using a range of neutral density filters and corrected for the background absorption of the substrate through use of a reference without the presence of the film. Raman spectroscopy was carried out using the spectrometer described above, with appropriate background subtraction. The background signal from a Triton X-100/water mixture of the same concentration as that used to form the surfactant-stabilised aqueous suspension has been subtracted from the spectrum from the suspension presented in Fig. 2(a). Likewise, background originating from a bare glass slide has been subtracted from that of the few-layer graphene (FLG) and MoS_2 (Fig. 2(c) films deposited on glass and the vdWHs presented in Fig. 3(b). Transmission electron microscopy was undertaken on films deposited on holey carbon grids using a JEOL 3100 microscope operating at beam voltage of 200 kV.

Film sheet resistance was measured using a home-built four probe device consisting of spring-loaded stainless steel contacts arranged in a van der Pauw geometry. A Keithley 2420 3A Source-Meter was used as a current source with voltage measured with a Keithley 2000 Multimeter. Transmittance corresponding to the region probed in each four-point measurement was found using the calibrated flatbed scanner, as described above. The FLG films were annealed under inert (argon) atmosphere in a tube furnace (Carbolite CTF 12/65/550) at various fixed temperatures (100, 200 and 300 °C) for 24 hours in order to improve conductivity. Transmittance and sheet resistance were measured after each anneal, with the samples cooled to room temperature and under ambient atmosphere. Conductivity data were derived from sheet resistance with nominal film thickness determined by assuming 2.3% light absorption per graphene layer[51] and a turbostratic interlayer spacing[52] of ~0.35 nm.

2.4 Sustainability

Our technique is specifically developed for aqueous surfactant-stabilised suspensions, eliminating the need for hazardous organic solvents at this stage. It is also possible to use biodegradable surfactants to produce these suspensions. The separation solvent, DCM, used to obtain the data presented in this paper, was recycled for further use using a rotary evaporator (Heidolph Laborota 4001).

3 Results and discussion

3.1 Liquid interface deposition

Surfactant-stabilised aqueous suspensions of thin (predominantly monolayer to few layer) platelets of a chosen 2D material were used as precursors for film and vdWH deposition. The suspensions were produced by a common, rapid approach for all the 2DLMs studied, as described in the Experimental section, obviating the need for specific liquid phases[53] and protocols[27] for each material. Triton X-100 was chosen as a low-cost, readily available surfactant, although the approach outlined can be readily modified to accommodate a broad range of common surfactants (see SI, Fig. S6).

To facilitate the LID process, the precursor suspension of 2DLM platelets was added to a centrifuge tube containing a 'separation solvent'. The separation solvent was chosen such that: (1) it is immiscible with, and denser than, the aqueous suspension; (2) it has a high partition coefficient such that the

surfactant prefers to be in the separation solvent to the aqueous phase; (3) the surfactant can be readily removed from the separation solvent enabling it to be re-cycled and re-used. In the experiments reported in this work, dichloromethane (DCM) was selected as meeting these conditions, with the partition coefficient, $K_{D/W}$, of Triton X-100 between DCM and water measured to be 220 ± 70 (in preparation, Finlay R. Dover, A. R. S., M. S., M. R. C. H.). In principle, any solvent/surfactant which meets the criteria described should be suitable for LID. This mixture is then centrifuged or left to settle *via* gravity (SI, Fig. S7), after which a thin film of 2DLM platelets is formed at the interface of the DCM and aqueous phase.

Our proposed mechanism for the assembly of 2DLM platelets at the liquid–liquid interface is shown schematically in Fig. 1(a). A detailed investigation into the mechanism is not within the scope of this work, and forms part of a future study. However, we note a key feature: removal of surfactant from the platelets of two-dimensional material brought about by surfactant partitioning into the separation solvent stabilizes assembly at the high energy water–DCM interface. Evidence for surfactant removal is presented below, but it would be expected that if it remained bound to the 2DLM platelets they would be less likely to become pinned to the liquid–liquid interface.[54] It has been suggested that assembly of 2DLMs at organic/aqueous interfaces is thermodynamically driven by interfacial energy minimisation.[12,29,54] In particular, interface stabilization occurs when the surface energy of the few-layer platelets exceeds that of the organic phase, with the sum of the interfacial energies between the 2DLM and each liquid phase being lower than that of the pristine organic–aqueous interface.[29] Assuming a universal surface entropy of ≈29 mJ m^{-2} at room temperature,[55] the (size and defect dependent[56]) room temperature surface energies of the 2DLMs used in this study – FLG (≈61–71 mJ m^{-2}),[55,56] MoS_2 (≈71–80 mJ m^{-2}),[55] WS_2 (≈82 mJ m^{-2})[57] – all lie between that of DCM (≈57 mJ m^{-2})[58] and water (≈101 mJ m^{-2})[55] and lead to similar reductions in interfacial surface energy upon their segregation to the DCM–water interface.

Film deposition is shown schematically in Fig. 1(b). To ensure reproducibility and consistency between films this process was automated by using a custom-built programmable dipping system (SI, Fig. S8 and video) such that insertion angle, dipping speed *etc.* could be fully controlled. However, it is also possible to carry out the process by hand. The dipping cycle may be repeated multiple times with the same material to build up thick films and with different materials to produce vdWHs, with no measurable damage to, or visible loss of, previously deposited material on subsequent dips.

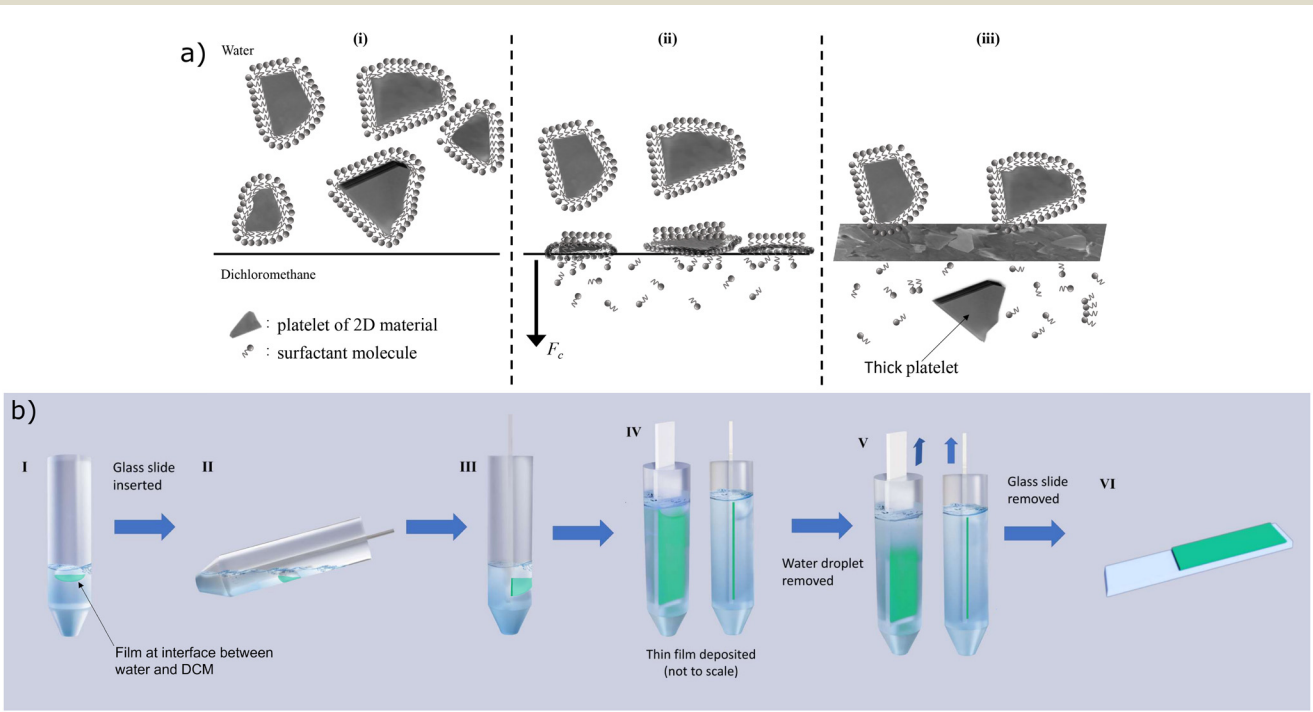

Fig. 1 (a) Proposed mechanism for formation of a 2DLM platelet film at the interface between the two immiscible liquids (water and dichloromethane for the data presented in this work) with the surfactant being removed from the 2DLM platelets into the denser liquid phase (dichloromethane). (i) State of system before centrifuging. (ii) Surfactant-stabilised 2DLM platelets migrate to the interface under the action of centripetal forces generated during centrifuging. (iii) Surfactant molecules and thicker platelets preferentially move across the interface into the denser solvent, while the 2DLM platelets assemble at the interface to minimise surface energy and form a film. (b) Illustration of the process used for the deposition of thin films and heterostructures. A centrifuge tube containing a 2DLM platelet film assembled at the interface between two immiscible liquids (I) (water and dichloromethane) was tilted, and the substrate inserted (II). The centrifuge tube was then returned to the upright (III). Further separation solvent was added to the tube, raising the interface and depositing the film onto the substrate (IV), after which the water droplet was removed (V) followed by the substrate (VI).

3.2 Versatility

The applicability of the LID process to a broad range of substrates is demonstrated in Fig. 2(a), which presents Raman spectra and optical images of FLG films deposited on copper, silicon, and (hydrophilic) glass. The films displayed a high degree of uniformity both optically and between regions selected for acquisition of the Raman spectra. Comparison between the Raman spectra of the thin films and that of the parent surfactant-stabilised aqueous suspension, also shown in Fig. 2(a), indicates similar characteristic Raman peaks, showing that no additional defects are introduced upon deposition. The continuity of the FLG films is demonstrated in Fig. 2(b), which shows a transmission electron microscopy (TEM) image of a graphene film deposited on a holey carbon grid (a TEM image for a MoS_2 film is shown in SI, Fig. S9). Although the film was produced using a single dipping cycle, and is therefore thin, it can be seen to be largely continuous, consisting of overlapping FLG platelets with very few pinholes present. Further images showing the large scale continuity of

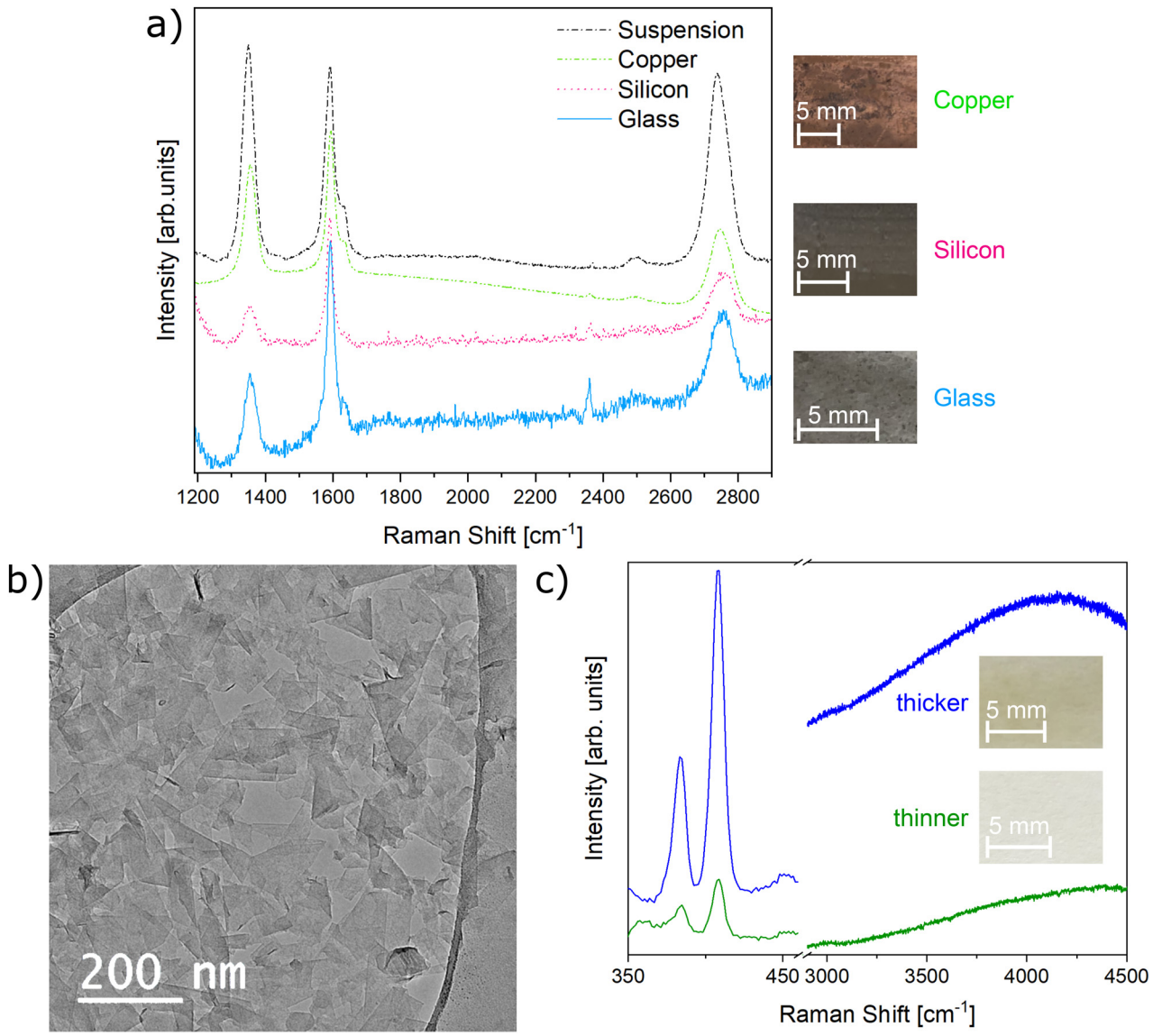

Fig. 2 (a) Raman spectra of few-layer graphene films deposited on different substrates and the surfactant-stabilised few-layer graphene aqueous suspension used as a precursor for deposition. Similar lineshapes between the few-layer graphene suspension and the films deposited on all substrates indicate no detectable increase in defect density upon formation of the film and film deposition. The data have been normalised with respect to the G peak, and offset vertically to allow for easier comparison. (b) Transmission electron microscopy (TEM) image showing a few-layer graphene film deposited onto a TEM grid *via* the LID method. The film can be seen to be largely continuous with only a few pinholes. (c) Raman spectra of two films of MoS_2 of different thicknesses, with the thinner sample shown in green and the thicker shown in blue. The $E_{2g}{}^1$ and A_{1g} peaks characteristic of MoS_2 can be clearly seen in both spectra, as can the A exciton peak. The position of the A exciton peak shows that these films are not behaving as in the bulk regime. The data have been offset vertically to allow for easier comparison.

the films are shown in the SI, Fig. S10. We find the continuous regions of the films produced by the LID process are substantially larger than those produced by Langmuir–Blodgett deposition from the same surfactant-stabilised suspensions by ourselves (SI, Fig. S11 and S12), and similar to those produced by other liquid–liquid interface deposition methods.[44]

The thickness of the films produced can be altered by altering the concentration of the surfactant-stabilised aqueous suspension of 2DLM, by repeating the dipping process multiple times, or both. The linear relation between number of dips and film thickness is demonstrated by the data presented in SI, Fig. S13. The minimum film thickness is, in principle, limited by the minimum thickness of platelets in suspension whereas the maximum film thickness which may be achieved in a single dip is limited by the suspension concentration. These factors are dependent on the 2DLM and the precise preparation method (*e.g.*, any size/thickness selection of the platelets in the suspension prior to deposition), however the LID method remains consistent for all 2DLMs and preparation methods.

Raman spectra of films produced using the multiple dipping approach are shown in Fig. 2(c) for two MoS_2 samples produced using different numbers of dips. No change in peak separation or relative intensity of the $E_{2g}{}^1$ and A_{1g} modes is observed (Fig. 2(c)). The separation of the $E_{2g}{}^1$ and A_{1g} lines is found to be 24 cm^{-1} in both films, corresponding to platelets of 4 to 5 layers,[59] indicating a weak interaction between the platelets as the film thickness is increased. A peak corresponding to the A exciton[60] can be seen at ~4300 cm^{-1} (1.8 eV), increasing in intensity in the thicker film.

It has previously been shown that exciton intensity decreases rapidly with the number of layers in thin films/plate-

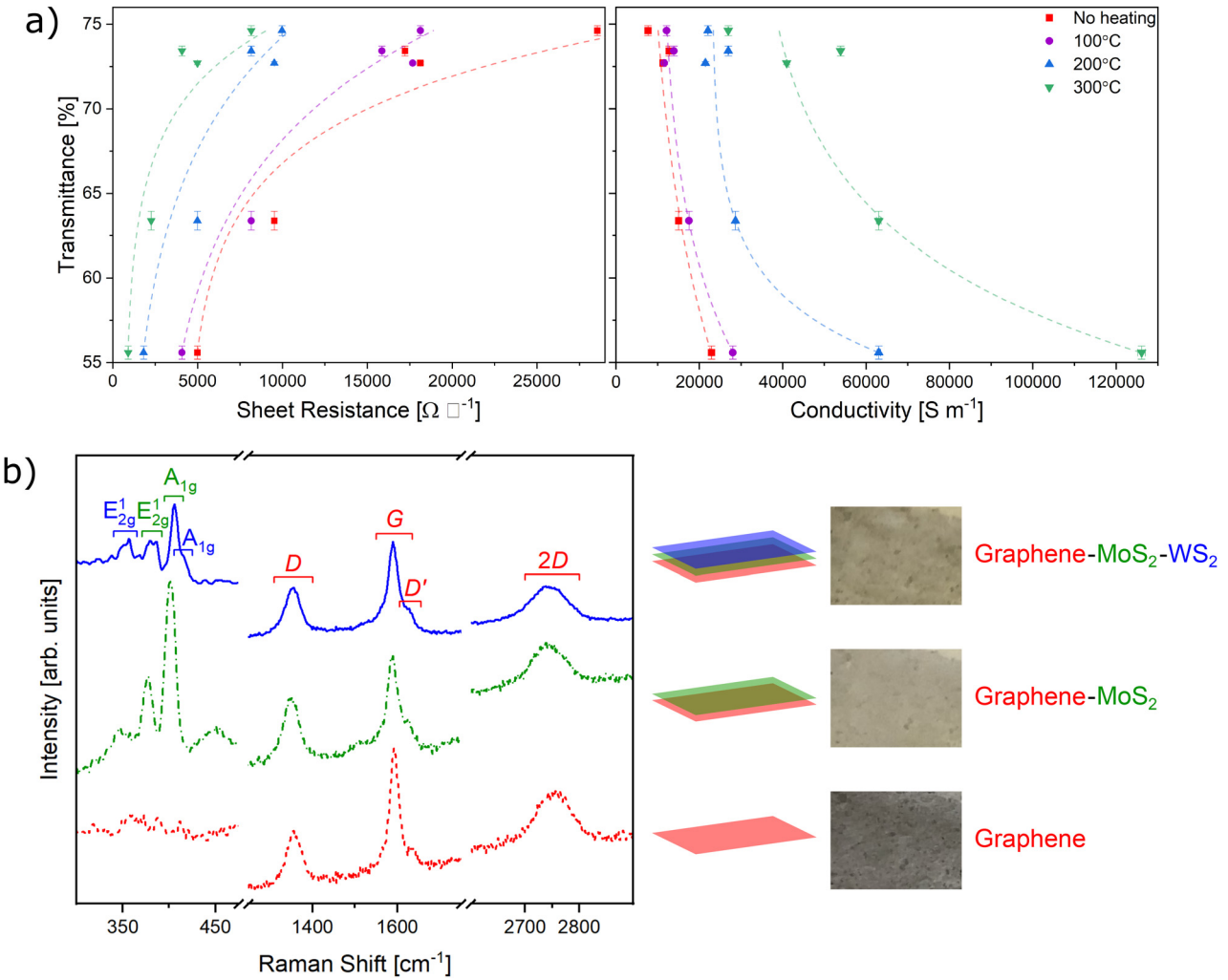

Fig. 3 (a) Sheet resistance and conductivity of few-layer graphene (FLG) films of different optical transmittance both as-deposited and after annealing for 24 hours at different temperatures. The dashed lines are guides to the eye. Error bars are standard errors. (b) Raman spectra of a FLG-MoS_2-WS_2 van der Waals heterostructure (vdWH) deposited on glass at each stage of fabrication. The red (dashed) data correspond to the first (FLG) layer, the green (dash-dot) data to a FLG-MoS_2 vdWH, and the blue data to a FLG-MoS_2-WS_2 vdWH. The data have been offset vertically to allow for easier comparison. Features from MoS_2, WS_2 and graphene are present in the Raman spectra of the final vdWH, indicating the vdWH fabrication has been successful. The photographs of the vdWH in each stage of fabrication are from the same area of the sample.

lets of MoS_2.[60] This phenomenon originates from a change in bandstructure as thickness increases due to interlayer coupling, which leads to a transition from a direct to an indirect band gap. Hence, in monolayer and few layer films in which the MoS_2 films are coupled sufficiently strongly, a decrease in exciton intensity with increasing thickness might be expected in the ultra-thin films studied here. The observed increase in intensity therefore is likely to reflect not just the presence of additional material but also that there is limited electronic coupling between material deposited in each dipping cycle, preserving few-layer behaviour.

3.3 Transparent conductive few-layer graphene films

To demonstrate the utility of the LID method, FLG films were deposited onto glass slides to form continuous transparent films with absorption which was found to vary weakly over visible optical wavelengths.[51] Sheet resistance was measured and found to decrease with transmittance, Fig. 3(a), as would be expected from the accompanying increase in film thickness,[61] and was found to range from 5–29 $k\Omega\,\square^{-1}$ for transmittances of 55–75%, which compares well to similarly produced films.[10] Films were annealed under an inert (argon) atmosphere at temperatures between 100 and 300 °C which resulted in an enhancement of conductivity, increasing with anneal temperature, where the maximum conductivity achieved was 126 kS m^{-1} for a transmittance of 55%. This behavior may be attributed to the removal of residual water and other contaminants which impede charge transfer between the FLG platelets and/or structural re-arrangement within the film leading to a greater contact between the platelets. Annealing films we produced by drop-casting surfactant-stabilised suspensions is found to lead to decomposition and not removal of surfactant. Hence, the presence and subsequent removal of residual Triton X-100 cannot explain the observed improvement of charge transport of the LID FLG films, and is consistent with surfactant removal during film formation. The relationship between transmittance and sheet resistance for these FLG films does not follow the typical relationship for thin metallic films, but instead shows percolative-like behavior as discussed in the work of De *et al.*[62] A detailed analysis is presented in the SI, section S4, Fig. S14 and S15.

3.4 van der Waals heterostructures

In order to demonstrate proof-of-principle production of a vdWH, Raman spectra were obtained at each stage in the fabrication of a FLG-MoS_2-WS_2 vdWH deposited on a glass slide. These are shown in Fig. 3(b) along with photographs obtained from the same region of the slide at each deposition step, which are indicative of a high degree of film uniformity. The spectra, obtained from a pure FLG film (red dashed line), a FLG-MoS_2 heterobilayer (green dash-dot line) and a heterotrilayer of FLG-MoS_2-WS_2 vdWH (blue line), can be understood to be a linear combination of spectra from each individual material. However, subtle changes can be observed to the graphene-related modes upon deposition of the subsequent TMDC layers. In particular, the deposition of MoS_2 to form the FLG-MoS_2 heterobilayer leads to a measurable change in the ratio between the FLG D and G peaks, I_D/I_G, from 0.48 to 0.77, which recovers somewhat to 0.58 after further deposition of a WS_2 layer. Likewise, there is a decrease in the ratio of the G to D′ peak intensities, which indicates that the cause is a loss of G band intensity. Similar changes to Raman spectra of graphene layers have been observed upon electrostatic doping[63] and in the assembly of other heterostructures,[64] which can originate from strain and/or doping.[65] The complex interplay of the effects of strain, doping, and thickness make the origin of the observed changes in Raman spectra difficult to isolate. However, the (partial) reversibility of the change to the graphene Raman spectrum would suggest that the origin of this behaviour (also observed in a FLG-MoS_2-FLG heterostructure, SI, Fig. S16) does not arise from damage or modification to the bottom FLG layer upon stacking of subsequent layers of TMDCs.

4. Conclusions

It has been shown that an approach to liquid–liquid interface assembly in which film assembly is coupled with removal of surfactant from a stabilised aqueous suspension of two dimensional material can be used to deposit thin films and van der Waals heterostructures of 2DLMs. This generic technique may be applied to 2DLM platelets which can be held in an aqueous surfactant-stabilised suspension and to a broad spectrum of solid substrates. The effectiveness of the technique has been demonstrated through the deposition of films of FLG and TMDCs on copper foils, natively oxidised silicon wafers, and glass slides; the formation of transparent, conductive FLG films with characteristics comparable to those reported in the literature; and vdWHs of FLG, MoS_2, and WS_2. The simplicity, scalability, generic nature, broad applicability and relatively low environmental footprint of LID opens a route for the routine use of 2DLM thin films and vdWHs in a range of applications.

Author contributions

A. R. S., M. Z., and A. G. M. M. performed sample deposition. A. R. S. optimised the deposition, designed the automated dipping machine, performed conductivity measurements, and took transmission scans. M. R. C. H. performed Raman measurements. A. R. S. and M. R. C. H. analysed the data. A. R. S., M. R. C. H., and M. S. wrote the initial draft of the manuscript and A. R. S. prepared Fig. 1–3. All authors edited and approved the manuscript. M. R. C. H. and M. S. conceived and supervised the project.

Conflicts of interest

There are no conflicts to declare.

Data availability

The data supporting this article have been included in this paper and in the supplementary information (SI). Supplementary information containing supporting data is available. See DOI: https://doi.org/10.1039/d6nr00608f.

Acknowledgements

The authors would like to thank Dr Lars-Olof Pålsson for the use of his UV-vis spectrometer. We would also like to thank Dr Alina Talmantaite and Prof. Budhika Mendis for their assistance with TEM imaging. The authors would also like to thank Mr Leon Bowen and the G.J. Russell Microscopy Facility at Durham University for assistance with this work. This work was funded by EPSRC Grant Number EP/T518001/1. The funder played no role in study design, data collection, analysis and interpretation of data, or the writing of this manuscript.

References

1 F. Schwierz, *Nat. Nanotechnol.*, 2010, **5**, 487–496.
2 F. Schwierz, *Nat. Nanotechnol.*, 2011, **6**, 135–136.
3 B. Radisavljevic, A. Radenovic, J. Brivio, V. Giacometti and A. Kis, *Nat. Nanotechnol.*, 2011, **6**, 147–150.
4 T. Hopf, K. V. Vassilevski, E. Escobedo-Cousin, P. J. King, N. G. Wright, A. G. O'Neill, A. B. Horsfall, J. P. Goss, G. H. Wells and M. R. C. Hunt, *J. Appl. Phys.*, 2014, **116**, 154504.
5 D. Rhee, D. Jariwala, J. H. Cho and J. Kang, *Appl. Phys. Rev.*, 2024, **11**, 021310.
6 X. Wang, L. Zhi and K. Müllen, *Nano Lett.*, 2008, **8**, 323–327.
7 A. G. Ricciardulli and P. W. Blom, *Adv. Mater. Technol.*, 2020, **5**, 1900972.
8 E. Varrla, C. Backes, K. R. Paton, A. Harvey, Z. Gholamvand, J. McCauley and J. N. Coleman, *Chem. Mater.*, 2015, **27**, 1129–1139.
9 T. Li, A. D. Pickel, Y. Yao, Y. Chen, Y. Zeng, S. D. Lacey, Y. Li, Y. Wang, J. Dai, Y. Wang, B. Yang, M. S. Fuhrer, A. Marconnet, C. Dames, D. H. Drew and L. Hu, *Nat. Energy*, 2018, **3**, 148–156.
10 S. De, P. J. King, M. Lotya, A. O'Neill, E. M. Doherty, Y. Hernandez, G. S. Duesberg and J. N. Coleman, *Small*, 2010, **6**, 458–464.
11 A. Matković, I. Milošević, M. Milićević, T. Tomašević-Ilić, J. Pešić, M. Musić, M. Spasenović, D. Jovanović, B. Vasić, C. Deeks, R. Panajotović, M. R. Belić and R. Gajić, *2D Mater.*, 2016, **3**, 015002.
12 S. J. Woltornist, D. Varghese, D. Massucci, Z. Cao, A. V. Dobrynin and D. H. Adamson, *Adv. Mater.*, 2017, **29**, 1604947.
13 T. Carey, J. Maughan, L. Doolan, E. Caffrey, J. Garcia, S. Liu, H. Kaur, C. Ilhan, S. Seyedin and J. N. Coleman, *Small Methods*, 2024, 2301654.
14 A. K. Geim and I. V. Grigorieva, *Nature*, 2013, **499**, 419–425.
15 K. S. Novoselov, A. K. Geim, S. V. Morozov, D.-e. Jiang, Y. Zhang, S. V. Dubonos, I. V. Grigorieva and A. A. Firsov, *science*, 2004, **306**, 666–669.
16 M. Yi and Z. Shen, *J. Mater. Chem. A*, 2015, **3**, 11700–11715.
17 L. Britnell, R. V. Gorbachev, R. Jalil, B. D. Belle, F. Schedin, A. Mishchenko, T. Georgiou, M. I. Katsnelson, L. Eaves, S. V. Morozov, N. M. R. Peres, J. Leist, A. K. Geim, K. S. Novoselov and L. a. Ponomarenko, *Science*, 2012, **335**, 947–950.
18 T. Georgiou, R. Jalil, B. D. Belle, L. Britnell, R. V. Gorbachev, S. V. Morozov, Y.-J. Kim, A. Gholinia, S. J. Haigh, O. Makarovsky, *et al.*, *Nat. Nanotechnol.*, 2013, **8**, 100–103.
19 J. Zhang, F. Wang, V. B. Shenoy, M. Tang and J. Lou, *Mater. Today*, 2020, **40**, 132–139.
20 Q. Wu, W. Wongwiriyapan, J.-H. Park, S. Park, S. J. Jung, T. Jeong, S. Lee, Y. H. Lee and Y. J. Song, *Curr. Appl. Phys.*, 2016, **16**, 1175–1191.
21 L. Hu, M. Chen, X. Fang and L. Wu, *Chem. Soc. Rev.*, 2012, **41**, 1350–1362.
22 H. A. Becerril, J. Mao, Z. Liu, R. M. Stoltenberg, Z. Bao and Y. Chen, *ACS Nano*, 2008, **2**, 463–470.
23 L. J. Cote, F. Kim and J. Huang, *J. Am. Chem. Soc.*, 2009, **131**, 1043–1049.
24 R. Tarcan, O. Todor-Boer, I. Petrovai, C. Leordean, S. Astilean and I. Botiz, *J. Mater. Chem. C*, 2020, **8**, 1198–1224.
25 L. Sun, G. Yuan, L. Gao, J. Yang, M. Chhowalla, M. H. Gharahcheshmeh, K. K. Gleason, Y. S. Choi, B. H. Hong and Z. Liu, *Nat. Rev. Methods Primers*, 2021, **1**, 5.
26 F. Chen, D. Varghese, S. T. McDermott, I. George, L. Geng and D. H. Adamson, *Sci. Rep.*, 2020, **10**, 18047.
27 J. Kim, D. Rhee, O. Song, M. Kim, Y. H. Kwon, D. U. Lim, I. S. Kim, V. Mazánek, L. Valdman, Z. Sofer, *et al.*, *Adv. Mater.*, 2022, **34**, 2106110.
28 S. Biswas and L. T. Drzal, *Nano Lett.*, 2009, **9**, 167–172.
29 S. J. Woltornist, A. J. Oyer, J.-M. Y. Carrillo, A. V. Dobrynin and D. H. Adamson, *ACS Nano*, 2013, **7**, 7062–7066.
30 X. Yu, M. S. Prevot, N. Guijarro and K. Sivula, *Nat. Commun.*, 2015, **6**, 7596.
31 Z. Cui, Z. Cao, R. Ma, A. V. Dobrynin and D. H. Adamson, *ACS Appl. Mater. Interfaces*, 2015, **7**, 16913–16916.
32 R. M. Clark, K. J. Berean, B. J. Carey, N. Pillai, T. Daeneke, I. S. Cole, K. Latham and K. Kalantar-zadeh, *J. Mater. Chem. C*, 2017, **5**, 6937–6944.
33 M. Padmanabhan, R. Meyen and K. Houghton, *Mater. Res. Express*, 2018, **5**, 095606.
34 J. Neilson, M. P. Avery and B. Derby, *ACS Appl. Mater. Interfaces*, 2020, **12**, 25125–25134.
35 J. Vujin, W. Huang, J. Ciganovic, S. Ptasinska and R. Panajotovic, *Langmuir*, 2023, **39**, 8055–8064.
36 S. T. McDermott, B. Ferland, J. Liu, P. Abeykoon, M. J. Joyce, S. Shuster, S. L. Suib and D. H. Adamson, *Synth. Met.*, 2025, **312**, 117866.
37 Y. Qi, N. Wang, Q. Xu, H. Li, P. Zhou, X. Lu and G. Zhao, *Chem. Commun.*, 2015, **51**, 6726–6729.

38 S. J. Woltornist and D. H. Adamson, *Ind. Eng. Chem. Res.*, 2016, **55**, 6777–6782.
39 C. M. Chapman, D. S. Srivastava, S. P. Ward, Z. Cui and D. H. Adamson, *ACS Appl. Mater. Interfaces*, 2024, **16**, 69901–69907.
40 C. D. Liyanage, R. M. A. Pererage, N. C. Vy, S. T. McDermott, D. Varghese, J. Fee, S. Xiao, M. A. Gultekin, S. L. Suib, A. Bazzi, S.-W. Lee and D. H. Adamson, *J. Membr. Sci.*, 2026, **748**, 125339.
41 N. M. Bandara, K. Umaiya, M. J. Joyce, C. E. Gouveia and D. H. Adamson, *J. Mater. Chem. B*, 2026, **14**, 5973–5982.
42 E. P. C. Higgins, S. G. McAdams, D. G. Hopkinson, C. Byrne, A. S. Walton, D. J. Lewis and R. A. W. Dryfe, *Chem. Mater.*, 2019, **31**, 5384–5391.
43 C. Chen, Y. Xie, J. Wang, Y. Lan, X. Wei and Z. Zhang, *Appl. Surf. Sci.*, 2021, **535**, 147737.
44 O. Cassidy, K. Synnatschke, J. M. Munuera, C. Gabbett, T. Carey, L. Doolan, E. Caffrey and J. N. Coleman, *npj 2D Mater. Appl.*, 2025, **9**, 2.
45 K. R. Paton, E. Varrla, C. Backes, R. J. Smith, U. Khan, A. O'Neill, C. Boland, M. Lotya, O. M. Istrate, P. King, *et al.*, *Nat. Mater.*, 2014, **13**, 624–630.
46 B. Coulter, *High-Performance & High-Capacity Centrifuges: Product Catalog.*, https://uk.vwr.com/assetsvc/asset/en_GB/id/39706114/contents/beckman-co%ulter-high-performance-centrifuge.pdf.
47 A. A. Green and M. C. Hersam, *Nano Lett.*, 2009, **9**, 4031–4036.
48 C. Backes, B. M. Szydłowska, A. Harvey, S. Yuan, V. Vega-Mayoral, B. R. Davies, P.-l. Zhao, D. Hanlon, E. J. Santos, M. I. Katsnelson, *et al.*, *ACS Nano*, 2016, **10**, 1589–1601.
49 S. E. Eppendorf, *Centrifuge 5804/5804 R Centrifuge 5810/5810 R Original Operating Instructions*, 1st edn, 2021.
50 S. De, P. E. Lyons, S. Sorel, E. M. Doherty, P. J. King, W. J. Blau, P. N. Nirmalraj, J. J. Boland, V. Scardaci, J. Joimel, *et al.*, *ACS Nano*, 2009, **3**, 714–720.
51 R. R. Nair, P. Blake, A. N. Grigorenko, K. S. Novoselov, T. J. Booth, T. Stauber, N. M. R. Peres and A. K. Geim, *Science*, 2008, **320**, 1308.
52 P. Kokmat, P. Surinlert and A. Ruammaitree, *ACS Omega*, 2023, **8**, 4010–4018.
53 J. Shen, Y. He, J. Wu, C. Gao, K. Keyshar, X. Zhang, Y. Yang, M. Ye, R. Vajtai, J. Lou, *et al.*, *Nano Lett.*, 2015, **15**, 5449–5454.
54 M. J. Joyce, S. T. McDermott, K. Umaiya and D. H. Adamson, *J. Colloid Interface Sci.*, 2024, **653**, 327–337.
55 A. Sehnal, S. P. Ogilvie, K. Clifford, H. J. Wood, A. A. Graf, F. Lee, M. Tripathi, P. J. Lynch, M. J. Large, S. Seyedin, K. Maleski, Y. Gogotsi and A. B. Dalton, *J. Phys. Chem. C. Nanomater. Interfaces*, 2024, **128**, 17073–17080.
56 A. Ferguson, I. T. Caffrey, C. Backes, J. N. Coleman and S. D. Bergin, *Chem. Mater.*, 2016, **28**, 6355–6366.
57 K. Godin, K. Kang, S. Fu and E.-H. Yang, *J. Phys. D: Appl. Phys.*, 2016, **49**, 325304.
58 PubChem, Dichloromethane, https://pubchem.ncbi.nlm.nih.gov/compound/6344#section=Surface-Tension, accessed: 08.05.2026.
59 C. Lee, H. Yan, L. E. Brus, T. F. Heinz, J. Hone and S. Ryu, *ACS Nano*, 2010, **4**, 2695–2700.
60 K. Mak, C. Lee, J. Hone, J. Shan and T. Heinz, *Phys. Rev. Lett.*, 2010, **105**, 2–5.
61 J. Liu, M. Notarianni, G. Will, V. T. Tiong, H. Wang and N. Motta, *Langmuir*, 2013, **29**, 13307–13314.
62 S. De, P. J. King, P. E. Lyons, U. Khan and J. N. Coleman, *ACS Nano*, 2010, **4**, 7064–7072.
63 A. Das, S. Pisana, B. Chakraborty, S. Piscanec, S. K. Saha, U. V. Waghmare, K. S. Novoselov, H. R. Krishnamurthy, A. K. Geim, A. C. Ferrari and A. K. Sood, *Nat. Nanotechnol.*, 2008, **3**, 210–215.
64 G. Froehlicher, E. Lorchat and S. Berciaud, *Phys. Rev. X*, 2018, **8**, 011007.
65 T. Vincent, V. Panchal, T. Booth, S. R. Power, A.-P. Jauho, V. Antonov and O. Kazakova, *2D Mater.*, 2018, **6**, 015022.